The Relationship of Transient Upper-Level Troughs to Variability of the North American Monsoon System

STEPHEN W. BIEDA III, CHRISTOPHER L. CASTRO, AND STEVEN L. MULLEN

Department of Atmospheric Sciences, and Institute of Atmospheric Physics, The University of Arizona, Tucson, Arizona

ANDREW C. COMRIE

Department of Geography and Regional Development, The University of Arizona, Tucson, Arizona

ERIK PYTLAK

National Oceanic and Atmospheric Administration/National Weather Service, Tucson, Arizona

(Manuscript received 19 February 2008, in final form 2 February 2009)

ABSTRACT

Relationships between transient upper-tropospheric troughs and warm season convective activity over the southwest United States and northern Mexico are explored. Analysis of geopotential height and vorticity fields from the North American Regional Reanalysis and cloud-to-ground lightning data indicates that the passage of mobile inverted troughs (IVs) significantly enhances convection when it coincides with the peak diurnal cycle (1800–0900 UTC) over the North American monsoon (NAM) region. The preferred tracks of IVs during early summer are related to the dominant modes of Pacific sea surface temperature (SST) variability. When La Niña–like (El Niño–like) conditions prevail in the tropical Pacific and the eastern North Pacific has a horseshoe-shaped negative (positive) SST anomaly, IVs preferentially track farther north (south) and are slightly (typically one IV) more (less) numerous. These results point to the important role that synoptic-scale disturbances play in modulating the diurnal cycle of precipitation over the NAM region and the significant impact that the statistically supported low-frequency Pacific SST anomalies exert on the occurrence and track of these synoptic transients.

1. Introduction

The frequent presence of upper-tropospheric lows in the subtropical North Pacific and North Atlantic during boreal summer is well documented (e.g., Riehl 1948; Kelley and Mock 1982). Of specific interest to the summer climate of North America are warm core upper-tropospheric lows that develop in the Gulf of Mexico and Atlantic in or near the tropical upper-tropospheric trough (TUTT) that, according to Whitfield and Lyons (1992), is a climatological mean summer circulation with an elongated shear axis (from northeast to southwest) in the upper troposphere. These lows often begin their westward progression from the TUTT into the core North American monsoon (NAM) region covering the southwest United States and northwest Mexico during the summer months. However, it is important that not every transient upper-tropospheric feature that occurs in the core NAM region develops in or near the TUTT region. For example, Pytlak et al. (2005) documented cold core upper-tropospheric lows that formed in the central Mississippi Valley and wrapped around the equatorward side of the subtropical ridge over the southwestern United States and were carried westward by the tropical easterlies across northern Mexico and Southern California. Irrespective of differences in point of origin or dynamic characteristics of these upper-level features, Douglas and Leal (2003) suggest that they appear to enhance the transport of low-level moisture north through the Gulf of California, a process now commonly termed a ‘‘gulf surge.’’ The low-level moisture coincident with

Corresponding author address: Mr. Stephen W. Bieda III, Department of Atmospheric Sciences, and Institute of Atmospheric Physics, The University of Arizona, Physics-Atmospheric Sciences Bldg., Rm. 542, 1118 E 4th St., P.O. Box 210081, Tucson, AZ 85721-0081.
E-mail: bieda@atmo.arizona.edu

DOI: 10.1175/2009JCLI2487.1

upper-level cooling subsequently destabilizes the atmosphere, resulting in a widespread convective outbreak in the core NAM region. They also found that precipitation is enhanced during this time within the metropolitan areas of Phoenix and Tucson, Arizona.

The NAM is a large-scale seasonal atmospheric circulation that generates between 50% and 70% of the annual precipitation during summer over the core NAM region (Carleton et al. 1990; Douglas et al. 1993; Higgins et al. 1997; Adams and Comrie 1997; Mitchell et al. 2002; Sheppard et al. 2002). Upper-level winds change from a westerly direction that transports air from the dry, cool eastern Pacific in late spring and early summer to an easterly direction that carries more humid air from the Gulf of Mexico into the NAM region in summer. The shift in prevailing wind results from the development of a monsoon ridge over the south-central United States (Watson et al. 1994a; Adams and Comrie 1997). However, as many studies have demonstrated (i.e., Hales 1972, 1974; Carleton 1986; Douglas et al. 1993), the mountains of the Sierra Madre effectively block low-level moisture of the Gulf of Mexico from being directly transported into the western half of the core monsoon region (defined as the ''tier 1 region'' in the North American Monsoon Experiment). Thus, the primary source of low-level moisture is from the eastern tropical Pacific and Gulf of California (Fig. 1), which can be provided via intermittent gulf surges (Maddox et al. 1995; Adams and Comrie 1997; Higgins et al. 2004; Rogers and Johnson 2007), or moisture from evapotranspiration sources in the Sierra Madre Occidental (SMO) (Watts et al. 2007).

Monsoon thunderstorms are linked to the diurnal cycle of convection. This process is driven primarily by daytime heating over elevated terrain. Higher potential temperatures in areas of elevated terrain, as compared to adjacent valleys and deserts, leads to upslope flow, moisture convergence, and the development of convective clouds over the mountains, typically in the late morning to early afternoon (e.g., Maddox et al. 1995). Thunderstorm development in the afternoon can be further enhanced by the presence of an upper-level cyclone (Fig. 2). Under favorable steering conditions, convection generated over elevated terrain during the early afternoon moves out over the hot deserts in the late afternoon or evening (e.g., Johnson et al. 2007). As a result, radiational cooling of the cloud tops leads to a steepened lapse rate and intensification of convection (Hales 1977). This is an important mechanism for rainfall during the monsoon, especially in the northern part of the NAM region (i.e., southwestern United States) where precipitation is more variable intraseasonally (Castro et al. 2007a).

Variability of monsoon precipitation at interannual and longer time scales is related to the positioning and

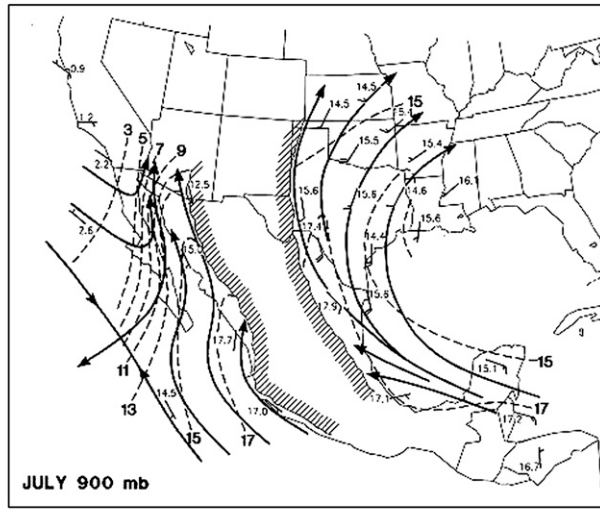

FIG. 1. July 900-mb streamline chart of wind patterns over the southern United States. Source: Douglas et al. (1993).

seasonal evolution of upper-level features, namely an upper-level monsoon/subtropical ridge (Carleton 1986; Carleton et al. 1990; Douglas et al. 1993; Watson et al. 1994a; Adams and Comrie 1997; Comrie and Glenn 1998; Grantz et al. 2007). If this ridge migrates anomalously far north or northeast of its climatological location—for example, the Four Corners region (the common joint corner for Arizona, Utah, Colorado, and New Mexico) during late July and early August—the core NAM region experiences enhanced upper-level easterlies and an increase in rainfall amounts and coverage. If the upper-level monsoon ridge is, instead, anomalously far south, the core NAM region experiences a weaker (or nonexistent) tropical influence and convection is normally suppressed. This relationship is out of phase with precipitation anomalies over the central United States (Carleton 1986; Carleton et al. 1990; Douglas et al. 1993; Watson et al. 1994a; Adams and Comrie 1997; Comrie and Glenn 1998; Grantz et al. 2007). The strength of the monsoon anticyclone during the monsoon onset period in the southwestern United States (late June/early July) is significantly related, in a statistical sense, to the state of the Pacific sea surface temperatures (SSTs) via a midlatitude atmospheric teleconnection response. If El Niño–like (La Niña–like) conditions prevail in the eastern and central tropical Pacific, and the eastern North Pacific has a horseshoe-shaped positive (negative) SST anomaly, an anomalous southward (northward) displacement of the monsoon ridge is likely to occur (Castro et al. 2001, 2007b).

Castro et al. (2007b) defined a combined Pacific variability mode (CPVM), considering two of the dominant rotated EOFs of global SST that reflect interannual and

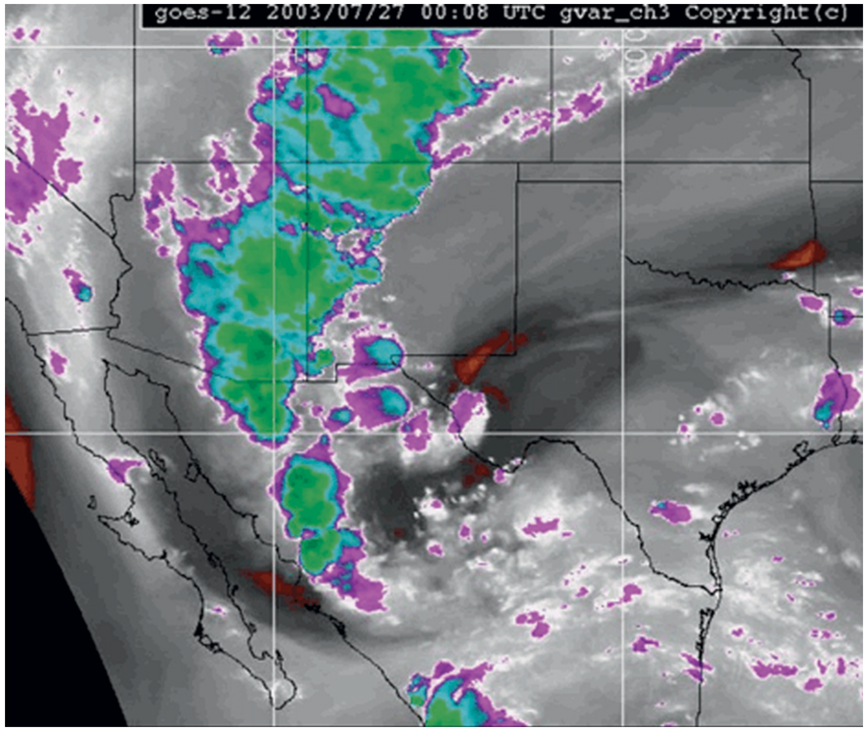

FIG. 2. Water vapor satellite image of a subtropical upper low, moving west from Texas toward Arizona, 1708 MST 26 Jul 2003. This low triggered a major severe thunderstorm outbreak across southeast Arizona.

interdecadal Pacific variability (see their Fig. 4). They found that, if the CPVM is positive (negative), NAM onset, as simulated by a regional climate model, is generally late (early) and summer precipitation is generally below (above) average within the NAM region. As they also note, the CPVM is quite similar to the pan-Pacific mode of Schubert et al. (2004) associated with dry and wet conditions in the central United States during the twentieth century. Interannual variability in the diurnal cycle of convection can dramatically change over relatively short distances in the southwest United States. Even more pertinent to the present work from Castro et al. (2007b), variations in a ''synoptic mode'' of convection (4–15 days) were found to exhibit a coherent relationship to the CPVM.

Understanding intraseasonal variability and its relationship to NAM precipitation is a research and forecasting challenge that has motivated several field campaigns, such as the North American Monsoon Experiment (NAME) (e.g., NAME Project Science Team 2004; Reyes et al. 1994). The westward progression of the aforementioned TUTT region features, such as easterly waves and upper-level lows, occur on the equatorward and west sides of the subtropical anticyclone where easterly and southeasterly flow exists respectively (Carleton 1986; Whitfield and Lyons 1992; Pytlak et al. 2005; Douglas and Englehart 2007). These features have a distinct influence on convection in the NAM region and came under intense study during NAME (NAME Project Science Team 2004). During 2003 and 2004, lower- and upper-level features were intensely monitored and tracked for research and forecast improvement on the hourly to interannual temporal scale (NAME Project Science Team 2004). A forecast operating center (FOC) in Tucson was created to support daily forecast operations (15 June 2004–30 August 2004), and forecasters were trained to observe specific features. One of these features was referenced as the inverted trough (IV), defined as a mid- to upper-level tropospheric low, detected by either water vapor or upper-air analysis, which was numbered and tracked as long as it was distinct and moving near the core monsoon region (Pytlak 2004). Inverted troughs were also targeted for intense observation periods when all National Weather Service (NWS) and Servicio Meteorológico Nacional (SMN) upper-air sites participating in NAME launched four to six radiosondes a day. A NOAA P3 aircraft also monitored possible Gulf of California moisture surges and the surrounding atmosphere (NAME Project Science Team 2004). These upper-level features pose a challenge for

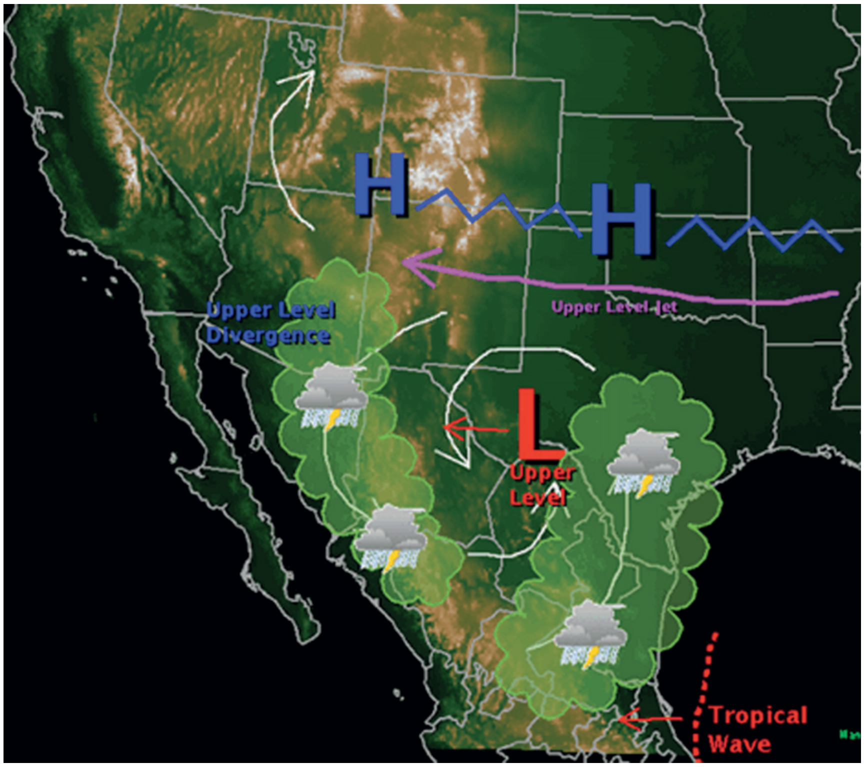

FIG. 3. Conceptual hypothesis of a subtropical upper-tropospheric low moving west into the North American monsoon regime, as adapted from Pytlak et al. (2005). The upper-level jet depicted in this figure is simply an enhanced easterly flow rather than a core of fast moving easterlies.

operational assimilation systems to analyze in real time with a high degree of confidence owing to their formation and propagation over data-sparse areas (e.g., Sierra Madre Occidental) and their modification by underlying terrain and deep convection. In these instances, output from high-resolution data assimilation systems, regional reanalyses (Mesinger et al. 2006), and remote sensing platforms (e.g., water vapor imagery) provide the means to track their evolution over many days.

Literature that focuses on the impact of transient synoptic systems is more limited in number and scope. Pytlak et al. (2005) applied potential vorticity (PV) thinking (James and Hoskins 1985) to hypothesize that two possible and distinct areas of upper-level divergence and midtropospheric upward vertical motion exist. The authors proposed that these areas are on both the leading (west) and trailing (east) quadrants of IVs (Fig. 3). These regions theoretically favor positive differential vorticity advection given a westward propagating feature. Pytlak et al. further hypothesized, and Douglas and Englehart (2007) later found, that upper-level cooling can also be expected from these transient IV features. Through this dynamical mechanism, upper-level systems can play critical roles in organizing mesoscale convective systems (MCSs). Douglas and Englehart further concluded that IVs were, on average, the dominant transient feature of the NAM region. These transient IVs were also classified by their work into warm (500-hPa trough temperatures $>-6°C$), neutral ($-7°C$ to $-8°C$), or cold ($<-8°C$). From this classification they determined that 62% of all inverted troughs were warm core, 30% were neutral, and 8% were cold core. Although this classification method may be somewhat simple and arbitrary, they did note differences in the physical characteristics of ‘‘warm’’ and ‘‘cold’’ IVs. A majority of these systems follow the dynamical and structural characteristics of TUTT features as found by Whitfield and Lyons (1992) with classifications that could be considered ‘‘neutral’’ or ‘‘warm’’ core. It is stressed by Douglas and Englehart (2007), however, that not all of these systems may have been detected at the 500-mb level. Systems of this classification were found to be midlevel manifestations of moderate or strong low-level tropical waves that were crossing the Mexican Plateau from the Gulf of Mexico, according to Douglas and Englehart. The ‘‘cold’’ IVs produce more precipitation on their forward flanks as they approach the core region of the NAM region and have structure and dynamics akin to midlatitude wintertime systems. Though much fewer in number, on average, these types of IVs can sometimes become cut off from both the polar westerlies and tropical easterlies and supply the forcing mechanism for catastrophic amounts of monsoon rainfall. A good example of this type of event would be one that occurred on 27–31 July 2006 when Tucson, Arizona, experienced a serious flooding event underneath a cutoff upper-level disturbance (Magirl et al. 2007). This system was an upper-tropospheric low that moved down the east side of the monsoon ridge and became cut off over the state of Arizona for four days. This event produced 265 mm during 3 days (a rainfall depth with an estimated 1000-yr recurrence) and caused major damage in Sabino Canyon, a popular local recreation area.

The NAME works of Pytlak et al. (2005), and Douglas and Englehart (2007) on the dynamics and climatology of IVs over the NAM region, leave unanswered questions concerning operational forecasting. For example, how does the passage of transient IVs influence the diurnal cycle of precipitation, a dominant temporal band of summertime convection over the NAM region? How does the phase of intraseasonal and interannual low-frequency modes (e.g., SST forcing) impact the occurrence of synoptic-scale transients? These are two questions that warrant better inferences of physical processes thorough statistical quantification. This paper addresses these two questions from a statistical perspective, and it takes advantage of datasets not yet applied in toto to upper-level IVs.

The outline for this paper is as follows: Section 2 describes the regional geographical definitions based upon those provided by the North American Monsoon Experiment literature. These definitions are chosen because of the size of influence and scaling of mesoscale and synoptic-scale features. An overview of the key geography is also given to help understand the weather and climate of the NAM region. The datasets and the methodology of analysis are also described there. Section 3 establishes that convective activity during specific hours of the diurnal cycle is enhanced by passage transient IVs. Section 4 demonstrates the importance of interannual Pacific SST variability on the frequency and passage of transient IVs. Discussion and conclusion are given in section 5.

2. Data used

a. Regional definition

The first region of interest is defined by the domain boundaries 20°N, 35°N, 105°W, and 120°W and is known as the ''tier 1 region'' (NAME Project Science Team 2004). The placement was chosen so as to maintain consistency with Moore et al. (1989) and Whitfield and Lyons (1992). The second domain of interest is defined by the domain boundaries 10°N, 40°N, 90°W, and 120°W and is known as the ''tier 2 region'' (NAME Project Science Team 2004). The interaction of the synoptic upper-level low feature and topography of the region (Figs. 2 and 3) is quite complex with the elevation being highly variable. In the region used, the area has major mountain ranges and isolated mountain peaks, complex coastal geometries, warm inland seas (e.g., Gulf of California), and strong SST differences separated by narrow peninsulas.

b. Datasets

1) CLOUD-TO-GROUND LIGHTNING DATA

The National Lightning Detection Network (NLDN) provides cloud-to-ground (CG) flash and stroke density for the contiguous United States and adjacent environments. Starting in 1996, the NLDN has undergone a series of improvements that has improved its accuracy in detecting lightning. The measured NLDN flash and stroke detection efficiency in southern Arizona was nearly 95%, with the remaining 5% not detected due to subsequent strokes of the same initial stroke family (Biagi et al. 2007). This is comparable to the nearly 90% detection efficiency for the remainder of the contiguous United States (Cramer et al. 2004). The high temporal and spatial resolution of CG lightning data make them extremely valuable for tracking convection and serving as a proxy for monsoon precipitation, especially over data-sparse regions (Tapia et al. 1998; Underwood and Schultz 2004).

The NLDN data, obtained courtesy of Vaisala, Inc., were used in this study to track CG lightning strikes each hour within a domain bounded by 27.5°N, 40°N, 100°W, and 120°W. This region is selected to be as close to tier II as possible, though the southern portion had to be reduced owing to data constraints. Data for this study were available for the 10 warm seasons (1 June–30 September) of 1996–2005. Over the study domain, the temporal precision is 10^{-3} seconds and location precision is approximately 10 m (K. Cummins 2007, personal communication). Although the NLDN is quite accurate throughout the United States and Canada, the same cannot be said for Mexico and Central America. Murphy and Holle (2005) report that the NLDN efficiency diminishes below 50% south of 27.5°N because of a lack of detection equipment in Mexico (see their Fig. A1). For that reason, the southern boundary was held at 27.5°N to ensure that the majority of the lightning strikes in northern Mexico are counted. It should be further noted that, because of this decrease in detection efficiency, the results presented in this paper south of the United States/Mexico border may be more significant than shown.

2) North American Regional Reanalysis

The North American Regional Reanalysis (NARR) uses the National Centers for Environmental Prediction (NCEP) Eta Data Assimilation System (EDAS), which began operation in April 2003, to generate 3-hourly fields on a 32-km grid for the North American continent and adjacent ocean regions (Mesinger et al. 2006). Analyses are available starting 0000 UTC 1 January 1979 to present. Despite having a much shorter data period than is available for the NCEP global reanalysis dataset (Kalnay et al. 1996), NARR fields have a higher spatial and temporal resolution that correspond more closely to the temporal signal of the diurnal cycle and the spatial interactions with the complex terrain. Both time scale and boundary layer conditions exert a strong influence on convective forcing in the NAM region (Maddox et al. 1995; Castro et al. 2007a). The time frame used to identify transient inverted troughs was the period from 15 May to 30 September that includes the onset (15 June) and decay (30 September) of the monsoon for the tier II region.

It is important, however, to acknowledge shortcomings of using NARR. The first, and what is considered fundamentally important, flaw is that NARR inaccurately overestimates the strength of the Gulf of California low-level jet associated with gulf surges (Mo et al. 2005; Castro et al. 2007a). While the NARR fields offer clear advantages over the NCEP global reanalysis, it was felt that supplemental analyses should be consulted as a consistency check on our initial NARR-based interpretations. Best-track reanalyses from the Colorado State Tropical Prediction Center (available online at http://www.weather.unisys.com/hurricane/e_pacific/) were used to make certain that tropical storms or hurricanes were not inadvertently labeled IVs. The U.S. Daily Weather Maps Project (available online at http://docs.lib.noaa.gov/rescue/dwm/data_rescue_daily_weather_maps.html) and, for dates after 1 December 1998, the NOAA National Weather Service Storm Prediction Center online map archives (available online at http://www.spc.noaa.gov/obswx/maps/) provided access to analyses with plotted radiosonde data. Thus, these two datasets helped provide a check on the veracity of the NARR analyses. Geostationary Operational Environmental Satellite (GOES) West IR and water vapor imagery for dates after 1997 were obtained from the Earth Observing Laboratory (available online at http://data.eol.ucar.edu/) portal of the National Center for Atmospheric Research to help manually observe and identify rotation centers of some upper-level vortices.

3. Analysis methodology

a. Construction of an inverted trough climatology

Manual interpretation of NARR analyses of geopotential height at four isobaric levels (250, 300, 500, 700 hPa) and temperature and relative vorticity at one level (500 hPa) is the primary means for identifying IVs. Three consecutive analysis times were simultaneously scrutinized for distinguishable upper-tropospheric (300 hPa) troughs that possessed clear temporal continuity over all maps with no distinction of the trough's core temperatures. If a temporally continuous feature was not found aloft, the midlevel maps (500 hPa) were next screened, followed by the low-level maps (700 hPa). If no distinguishable closed geopotential height contour center or geopotential height curvature (i.e., <975 dm at 300 hPa, <582 dm at 500 hPa, <318 dm at 700 hPa) signifying a trough could be confidently identified in the geopotential analysis sequence at any level, that date–time period was classified as a *no-trough* event. Furthermore, if the feature in question was determined to be a tropical cyclone or tropical wave through the use of the Unisys hurricane dataset, the date–time period would also be classified as a *no-trough* event. On the other hand, when an IV was identified, the latitude–longitude of its center was pinpointed from the location of the 500-hPa vorticity maximum and through qualitative screenings of IR and water vapor satellite imagery via identification of a cyclonic circulation (as demonstrated in Fig. 2). Analysis of satellite imagery is typically done by operational weather forecasters during the monsoon, as little to no upper-air sounding data over northern Mexico exist. Using this methodology, latitude–longitude points of IVs were digitally cataloged on a 3-hourly basis, as were dates and times without IVs. Climatology of IVs for the NAM region can be readily constructed from the inventory.

Composites of CG strike density for periods with and without IVs are generated as follows. Times that had an IV pass within a domain bounded by 23.5°N, 40°N, 100°W, and 120°W (as opposed to 27.5°N on the southern border) are classified as *IV days*, while times that do not are considered *non-IV days*. The boundary is expanded southward to ensure that the influence of the IVs (meridional scales of roughly a few hundred kilometers) centered somewhat south of 27.5°N is included. The approach further stratifies the NLDN data into 24-h bins with respect to changes in the diurnal cycle of convection and to establish whether IV days are significantly different from non-IV days. A Student's *t* test difference of means is used to test for local significance. Field significance tests (e.g., Livezey and Chen 1983) are also performed for the spatial autocorrelation of geopotential height and vorticity, considering significance at the 99% level, using 500 realizations with 1218 degrees of freedom (122 days $\times$ 10 yr $-$ 2).

The IV and non-IV days are used to define composites of the NARR accumulated precipitation dataset. The NARR dataset has a 3-h time sampling and accumulates precipitation over this time period. To maintain consistency between the NLDN dataset and the NARR dataset, the NLDN dataset is summed over the same three hours (i.e., 18 + 19 + 20 UTC for NARR precipitation ending 21 UTC). The null hypothesis testing is the same (i.e., *t* test difference of means, field significance test) in determining the difference between IV days and non-IV days using 99% significance and 1218 degrees of freedom.

b. Interannual variability of IVs

Composites of IV tracks are classified by the phase of interannual Pacific SST variability, specifically the sign of the CPVM (Castro et al. 2007b). Recall that, if this index is positive (negative), NAM onset typically is late (early) and precipitation amounts during the NAM season are statistically below (above) average within the core NAM region. The period analyzed in the Castro et al. (2007b) was 1950–2002, whereas our study is limited to 1980–2002. The phase of the CPVM for each year from 1980 to 2002, which is repeated in Table 1 for convenience, shows 9 negative and 10 positive seasons.

The seasonal evolution of IV tracks for the two CPVM phases is based on 30-day moving averages. Composites are computed for overlapping 30-day periods in 15-day increments, starting on Julian day 155 (4 June) and continuing for days 170 (19 June), 185 (4 July), 200 (19 July), 215 (3 August), and 230 (18 August), consistent with the methodology of Castro et al. (2001, 2007b). These periods were deemed important to track changes in the transient features as the monsoon progresses over the core monsoon region. The Student's *t* test is used to test for local significance (95%), and field significance (e.g., Livezey and Chen 1983) is assessed assuming 17 degrees of freedom (9 negative years + 10 positive years – 2) and 500 realizations.

4. Results

a. Diurnal cycle

Warm season convection over the continents and coastal zones is marked by a strong diurnal signal (Wallace 1975; Zajac and Rutledge 2001). The NAM region is no exception. Over Arizona for example, the higher terrain of the Mogollon Rim and White Mountains experiences a diurnal maximum during midafternoon hours, whereas the lower terrain of central and western Arizona experiences its maximum during the early and late evening hours (Hales 1977; Balling and Brazel 1987; King and Balling 1994; Watson et al. 1994b; Maddox et al. 1995). It is hypothesized by Pytlak et al. (2005) that the changes in upper-level divergence and static stability associated with transient IVs could strongly affect the diurnal signal. Hence, it is of value to quantify the role that IVs have in affecting the diurnal cycle throughout the core NAM region.

TABLE 1. Years in the 1980–2002 period comprising positive and negative years for the CPVM, as presented in Castro et al. (2007b). Negative (positive) years are associated with La Niña (El Niño) like patterns.

Negative	Positive
1981	1982
1984	1983
1985	1986
1988	1987
1989	1990
1999	1991
2000	1992
2001	1993
2002	1994
	1997

Figure 4 shows the 3-h evolution of hourly lightning density for the six times of 1800 UTC (1100 LST) to 0900 UTC (0200 LST), inclusive, hours that coincide with the NARR analyses. Results are normalized by the total days in the 10-season composite (1220) to units of km^{-2} h^{-1}. The daily convective cycle commences around 1100 LST (Fig. 4a) over the high terrain of New Mexico (Sacramento Mountains, Sangre de Cristo) and Arizona (Mogollon Rim, White Mountains). Convective activity reaches its peak diurnal values over these mountain regions three hours later (1400 LST, Fig. 4b). Lightning also peaks over the Santa Rita Mountains (southern Arizona) and the northern Sierra Madre Occidental (northeastern Sonora, Mexico), where the CG density increases tenfold between 1800 and 2100 UTC to its domain maximum of ~25 km^{-2} h^{-1} (e.g., Murphy and Holle 2005). Convection moves off the terrain by late afternoon, 1700 LST (Fig. 4c). It propagates eastward from the Sangre de Cristo range and westward or southwestward over Arizona and northern Sonora State in Mexico, consistent with prior analysis of radar echoes (e.g., Knievel et al. 2004, their Fig. 9). In most regions, the lightning count decreases markedly from late afternoon to early evening (Fig. 4d). Convection weakens, then dies as it approaches the

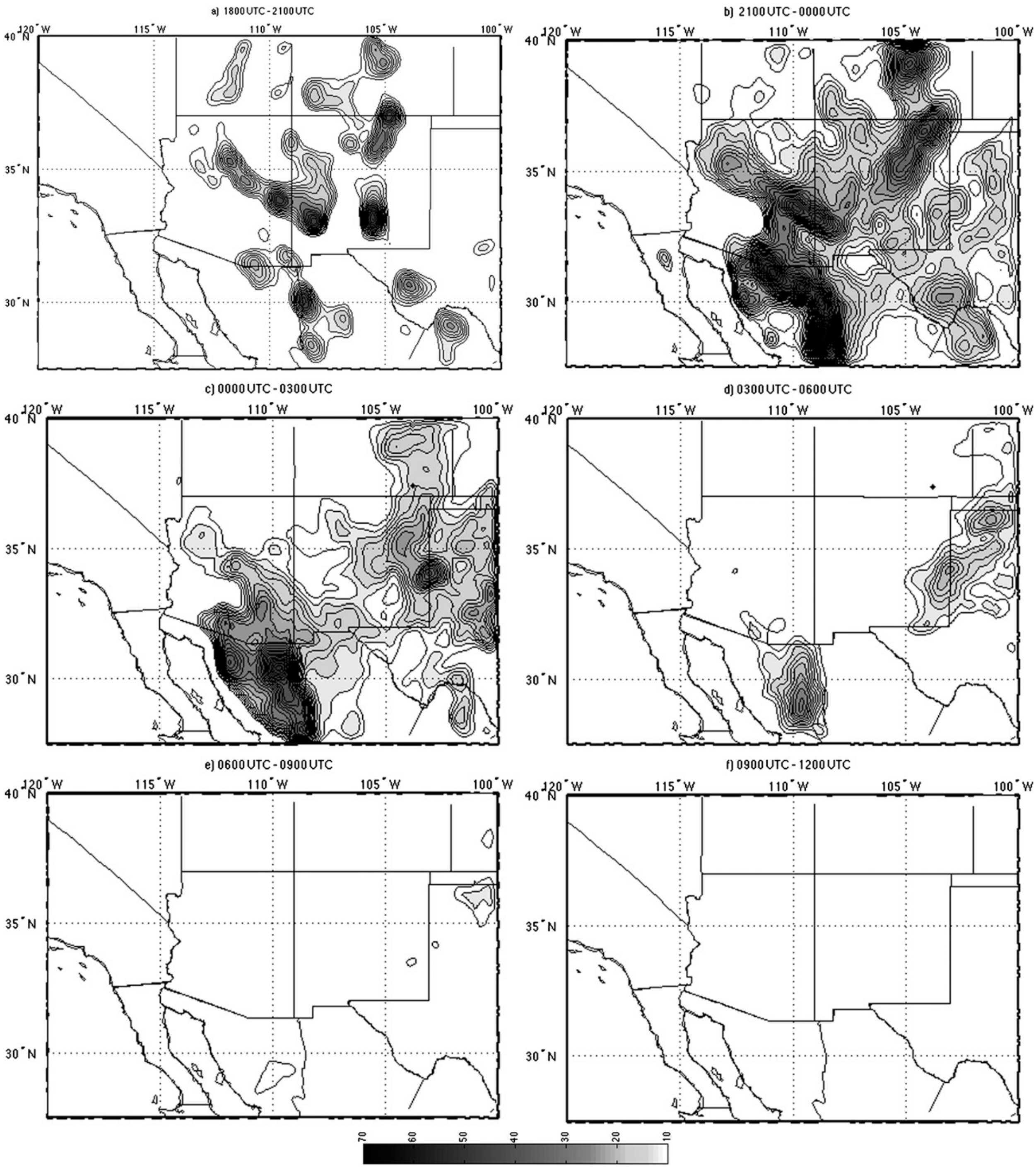

FIG. 4. (a)–(f) Normalized lightning climatology count km^{-2} (3 h)$^{-1}$ for the lightning region. Counts above 10 km^{-2} (3 h)$^{-1}$ shown. Hours UTC are noted within each figure caption.

Gulf of California and lower desert of Southern California during the evening hours from 2000 to 0200 LST. Domain-averaged CG flash density is a minimum during the early morning daylight hours (1200 and 1500 UTC, results not shown).

Figure 5 presents the difference in CG density count (km^{-2} h^{-1}) for IV days minus the non-IV days. Each composite shows field significance at the 99% level, which indicates that the presence of an IV has a strong impact on the likelihood of lighting. Despite accounting

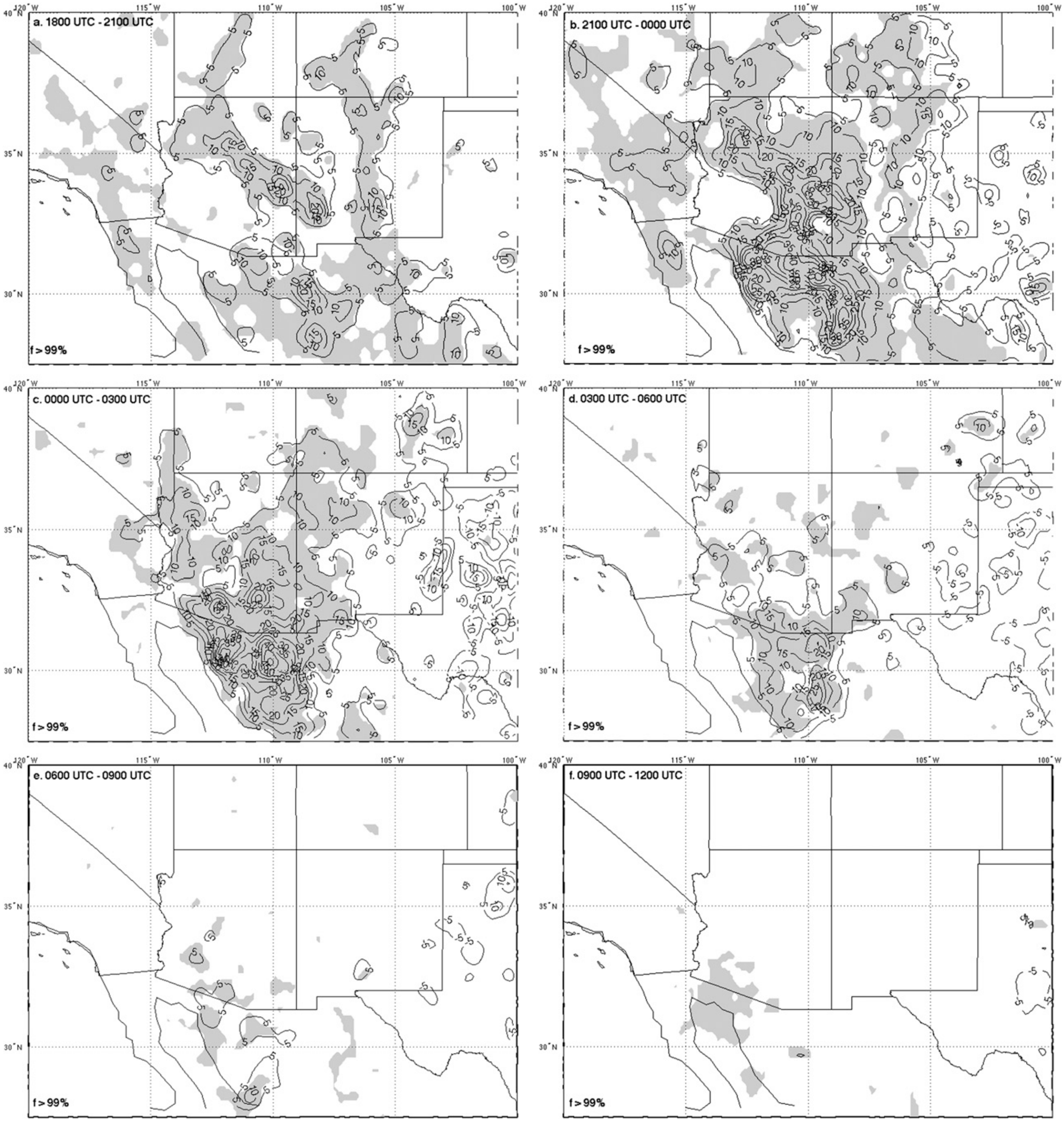

FIG. 5. (a)–(f) Lightning climatological difference between IV days minus non-IV days every 10 counts km^{-2} (3 h)$^{-1}$ for the lightning region. Stippling indicates regions of local significance at 99%. Hours UTC and field significance are noted within each figure caption.

for only 38% of all sample days, IV days account for the majority of total lightning strikes over Arizona and northern Sonora. The enhancement becomes significant by 1100 LST (Fig. 5a), with distinct maxima over the climatologically favored high terrain of the Mogollon Rim and SMO. The differences during midafternoon (Fig. 5b) grow and expand away from these ranges, consistent with the mechanisms advanced by Hales (1977), whereby convective activity is more likely to occur in the lower deserts of south-central Arizona and northwest Sonora due to steepened lapse rates and radiational cooling of cloud tops. Largest positive differences are centered over the southern portion of the SMO by early evening (0200 LST, Fig. 5d). Despite the small positive differences, the nighttime panels (Figs. 5e,f) indicate that local significance is essentially confined to extreme southwest Arizona, western Sonora, and the northern Gulf of California. These panels provide evidence of increased lightning counts enhanced in the western deserts of northwest Mexico and southwest Arizona during IV days.

Interpretation of the CG and NARR precipitation and precipitable water data provide some insight into the role played by transient synoptic IV in modulating precipitation. The enhancement of accumulated precipitation during IV days can be as large as 3 mm over the desert regions. Over some regions, such as the low deserts of southwestern Arizona, the enhancement occurs over a prolonged period (0000–0600 UTC). When precipitation is accumulated over the 24-h day, the enhancement on IV days over background non-IV days can add up to 6 mm over the low deserts. Mountainous areas, such as the Mogollon Rim, also have statistically significant enhancements of this magnitude. These results suggest that transient IVs are conducive for increased precipitation over the bulk of the NAM region as well as an increased presence of precipitable water versus climatology (Fig. 6).

In view of the strong signal evident in the CG data, it is of interest to examine how IVs impact precipitation. The 0–3-h precipitation accumulations from the NARR fields were used to examine this signal from a broad perspective (Fig. 7). Although there is agreement on where and when both the CG and NARR difference fields achieve local significance (Figs. 5 and 7), there is an apparent physical discrepancy between the two fields in a few key places. For example, the CG composite has a significant local enhancement of lightning activity during IV days at 2100 UTC in western Sonora, whereas precipitation input for the NARR assimilation has a meager (if any) signal. The same inconsistency continues throughout the later hours (e.g., 0000 UTC, 0300 UTC, etc.) over western Sonora. Moreover, we observe similar differences near the Arizona–Sonora border region between the CG data and composites based on the 1° Climate Prediction Center (CPC) precipitation product (results not shown), which is the precipitation input during the NARR assimilation. So the result of physical discrepancies is not surprising. Alternatively, the discrepancy between the NDLN and NARR may, in good part, reflect actual physical differences if virga was more prevalent over the low deserts. Unfortunately, we do not have a quantitative estimate by how much the ratio of CG to total precipitation varies between high terrain and the low deserts. However, thermodynamic reasoning suggests that virga should, indeed, be relatively more frequent underneath the high-based convection of low-desert convection. This raises the general issue of the joint assimilation of CG and precipitation data for semiarid environments, one that is beyond the scope of this paper. It also points to the value of using NDLN data to document thunderstorm activity over the NAM region.

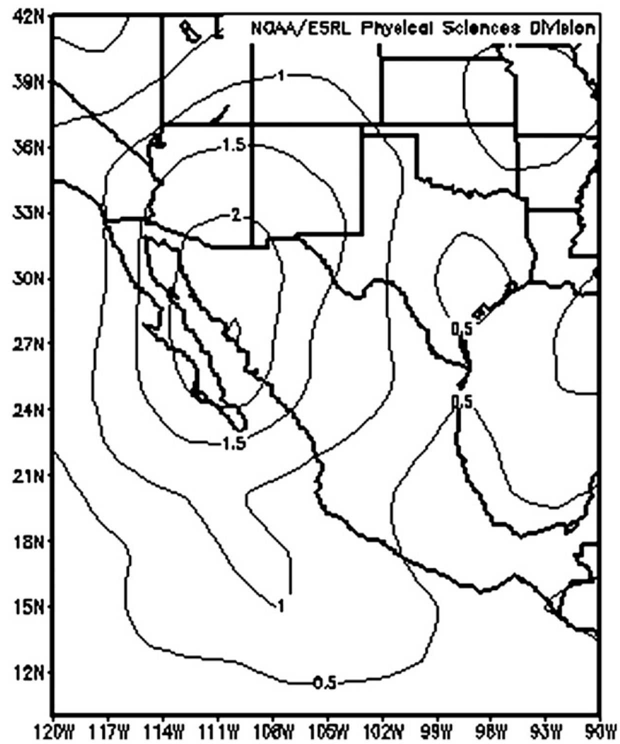

FIG. 6. (a)–(f) NARR precipitable water every 0.5 mm keyed to IV days, as compared against climatology.

b. Interannual variability

As already noted, the negative phase of the CPVM (see Castro et al. 2007b, their Fig. 4) is associated with a northward displacement of the monsoon ridge, an earlier monsoon onset, and wetter summer over Arizona, so it stands to reason that the occurrence of IV would be affected too. Therefore, it is of interest to quantify this relationship and estimate its statistical significance.

Climatological track densities were compiled to diagnose the evolution of the transient IVs during a ‘‘typical’’ monsoon season. Figure 8 gives the seasonal evolution of the climatological IV track density at 15-day intervals, standardized over 17 years. During the early onset period of the NAM season of 4–18 June (Fig. 8a), the total number of IVs averages only 1 per year per 15 days, a much lower frequency compared to the monsoon peak (late July–early August). The low value reflects the monsoon easterlies not being established in early June; by definition and experimental design, transient IVs over the region must track equatorward of the subtropical ridge, so the absence of easterlies

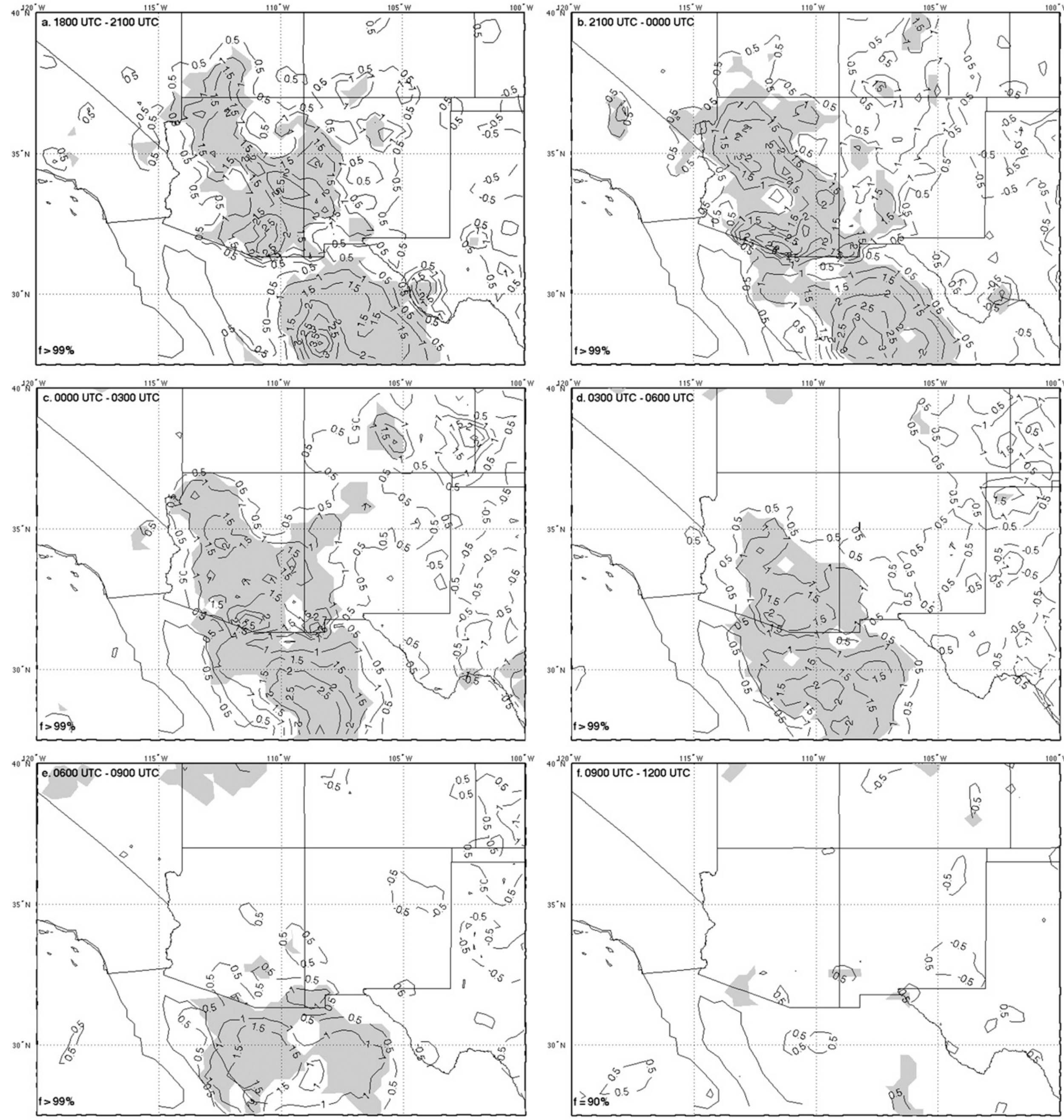

FIG. 7. (a)–(f) As in Figs. 4a–f but for NARR accumulated precipitation every 0.5 mm day^{-1}.

ensures no IVs. Despite the low values, a well-defined track axis is seen centered approximately along 22°N with maximum density near the mouth of the Gulf of California (Fig. 8a). The latitudinal variability in density is related in part to interannual (shown by the cooler colors) differences in the strength and position of the ridge. As the NAM develops and the easterlies become better established, the climatological track densities increase to their maximum value of about 2.8 IVs per year per 15 days from early July to early August (Figs. 8c,d). The maximum nudges northward, closer to the mouth of the Gulf of California. The shape of the track also changes from June to July, becoming more northwest–southeast oriented over southern Baja and sharper along its axis, in response to the 500-mb (Douglas et al. 1993) anticyclone moving its center from southeast Arizona to west-central Texas during the peak of the monsoon season. During the peak of the monsoon season

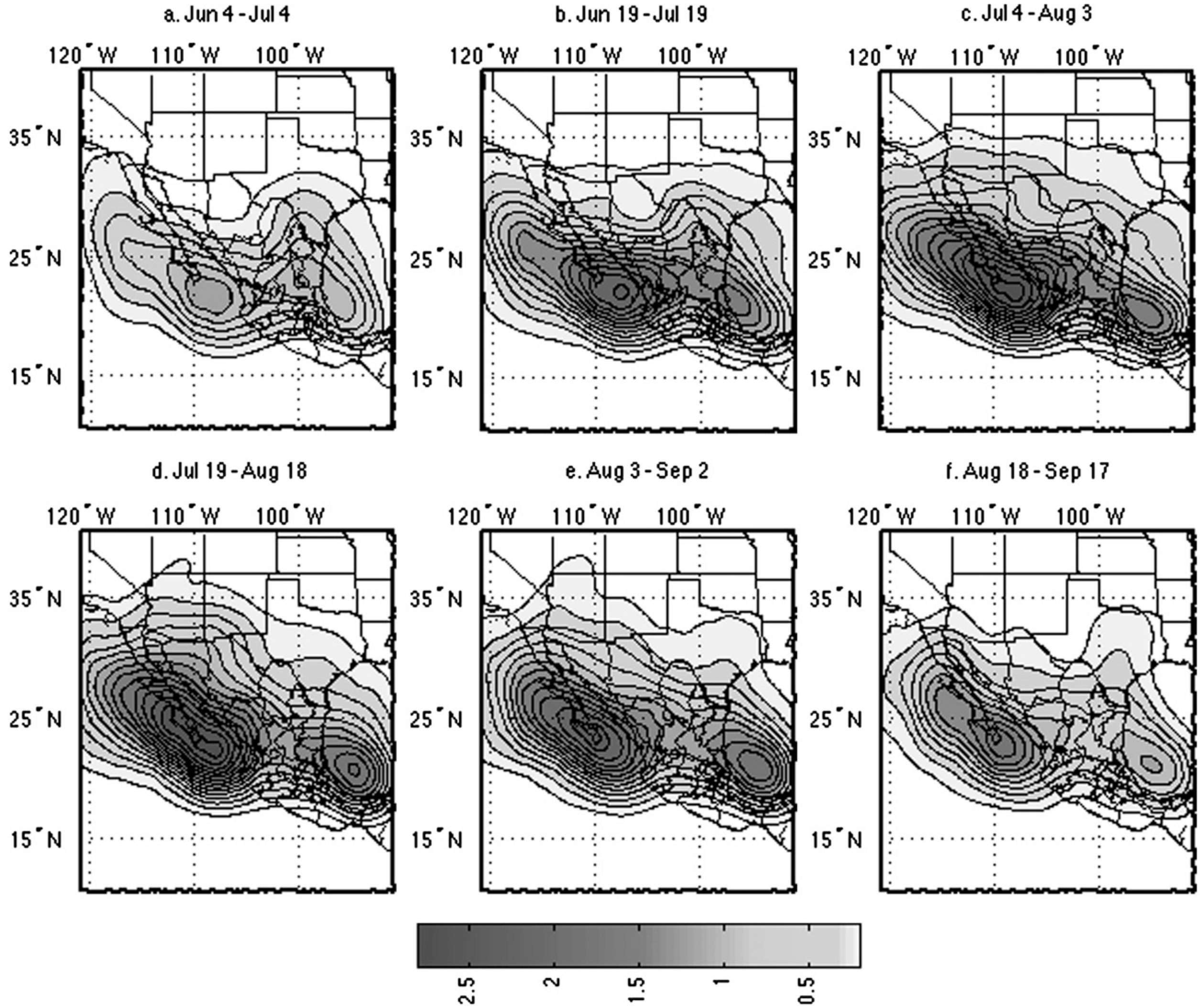

FIG. 8. (a)–(f) Track density climatology for all years within the NAME tier II region using a 30-day average of total IVs per 1° × 1° grid cell. A data density equation was used where 1 was the center and a radius of 1° from the center was considered 0. One degree is equal to approximately 4 times the grid spacing of NARR, which was near the limit of physically resolved wavelengths in the dataset (Pielke 2002). Dates are noted within each figure caption.

(July to mid-August, Figs. 8c,e), a secondary density maximum develops over the western Gulf of Mexico with peak values of 1.8 IVs per year (Fig. 8d). The primary maximum west of Mexico and secondary maximum east of Mexico are suggestive of two possibilities: either IVs develop in situ downwind of the Mexican Plateau or they impinge against the Plateau from the east, lose their identity over the elevated terrain, then reorganize and strengthen over the west coast of Mexico. Either possibility implies an important role for leeside cyclogenesis in the track and development of IVs (e.g., Zehnder 1993). As the summer monsoon wanes (18 August–17 September, Fig. 8f), track densities decline in number and retreat southward as the easterlies weaken and subtropical anticyclone begins its preautumnal equatorward drift.

A normalized difference of means IV track density between CPVM positive years and negative years (with associated local significance of 90% due to the use of subjectively analyzed data) is shown in Figs. 9a–f. Consistent with the increase in rainfall, when the CPVM index is negative (positive) there is a statistically significant increase in the number of transient IVs and a poleward shift of tracks during the monsoon onset and early part of the peak periods (Figs. 8a–d, late June through July). The regions that are most affected during the month of June are Texas, New Mexico, the Mexican states of Baja California Norte and Sur, and those

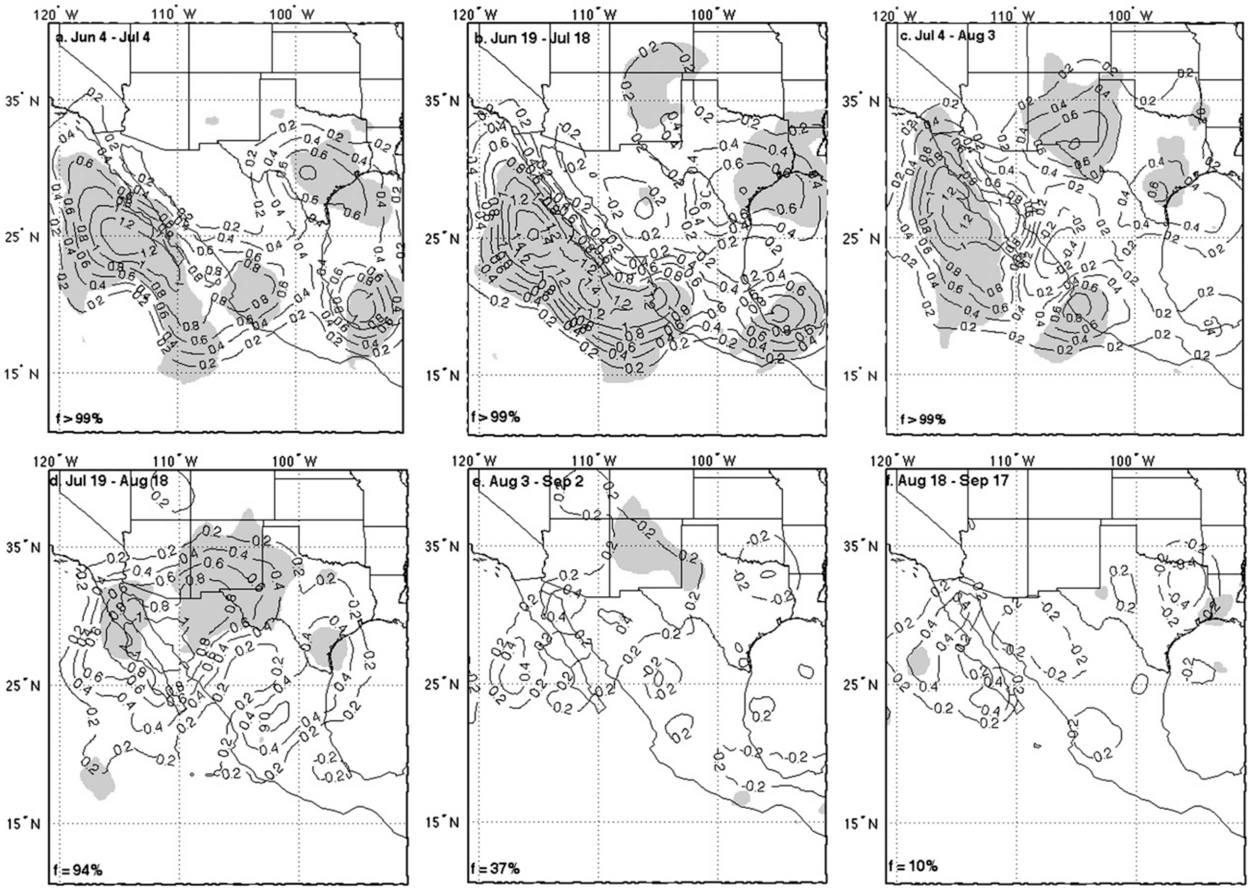

FIG. 9. (a)–(f) Climatological track density difference for CPVM negative years minus CPVM positive years within the NAME tier II region using a 30-day average. Dates and field significance are noted within each figure caption, with stippling indicating 90% local significance.

Mexican states along 20°–22°N. In early July the statistically significant enhancement shifts poleward into New Mexico, Texas, and off the west coast of Baja California. While in late July the statistically significant enhancement is primarily in the northern part of the tier II region, mainly in Arizona, New Mexico and Texas, this enhancement rapidly diminishes in August. These results are entirely consistent with the modeling results of Castro et al. (2007b) that, as mentioned, showed an enhancement in moisture flux convergence on a ''synoptic'' time scale of 4–15 days of the CPVM during July (Castro et al. 2007b, their Fig. 12).

5. Discussion and conclusions

An aim of this study was to determine whether transient IVs could either enhance or interrupt the diurnal cycle of convection within the study region. When all hours over 1220 days (from 1 June 1 to 30 September in 1996–2005) were analyzed, it was determined that lightning counts during the hours from 1800 to 0900 UTC were significantly different than IV days (453 days) vis-à-vis days that were not (747 days). As a trough could be located anywhere within the lightning region, as well as within 4° latitude south of it, this suggests that IVs can influence upper-level dynamics over a large area (i.e., $>10^2$ km). The findings support the conclusions by Douglas and Englehart (2007), suggesting that these transient IVs were indeed important and can enhance convective rainfall.

An enhancement of convection in the western deserts of Arizona during most of the statistically significant hours (e.g., 1800–0900 UTC) of lightning and precipitation was noted during the study. According to the conclusions of Douglas and Leal (2003) and Higgins et al. (2004), such an anomaly in the diurnal cycle, typically phase locked to topographic influence, is normally in response to increased moisture from gulf surge events. In Fig. 12 of Douglas and Leal (2003), it is interesting to note that a midlevel cyclonic circulation near the mouth of the Gulf of California aided the gulf surge. The surface response a day before and the day of the surge was an anomalously strong southeastern flow that extended the entire length of the Gulf of California. This is in agreement with the findings of Higgins et al. (2004) who concluded that "wet" gulf surges were associated with diffluent flow into the states of Arizona and New Mexico and anomalously strong easterly flow (i.e., easterly waves). Rogers and Johnson (2007) documented that a gulf surge during NAME was associated with not only Tropical Storm Blas, but a strong north–south inverted trough at 200 mb located over northern Mexico. It was noted by both Rogers and Johnson (2007) and Pytlak et al. (2005) that upper-level divergence associated with the inverted trough aided in the development of convection over the Sierra Madre Occidental. As a result, an MCS formed over the region, and, with the aid of Tropical Storm Blas, the environment was primed for a gulf surge (Higgins et al. 2004). Further, Johnson et al. (2007) noted another "strong" gulf surge on 23 July2004 that was due to an upper-tropospheric low. Given the conclusions of three prior studies that stated that gulf surges were possibly associated with upper-tropospheric lows, it is reasonable to conclude that the enhancement of lightning noted in Fig. 4c in the southwestern deserts of Arizona and northwestern Mexico is likely associated with the same factors. However, the present temporal and spatial resolution of upper-air data in Mexico makes it extremely difficult to forecast these events.

From a climatological standpoint, transient IVs tended to track over central Mexico and reach a maximum over the tip of southern Baja California (or the mouth of the Sea of Cortez). During CPVM negative years, though, transient IVs are more numerous during the months of June and July (by as much as one more IV per year) and take more northerly tracks. This likely resulted in more convection over the core monsoon region. Furthermore, knowing that the CPVM is negative could be an important climate diagnostic tool in determining whether the core NAM region will have an early onset as well as having more IVs and precipitation during the upcoming NAM season. Our future work will quantitatively test whether the CPVM may have value as a potential forecasting tool for NAM interannual variability. Also, detailed numerical modeling studies and/or climatological studies of IV events will be considered under different Pacific SST conditions to ascertain the relationship that these synoptic-scale features have to gulf surge events.

Acknowledgments. We acknowledge the assistance of Dr. Kenneth Cummins in providing the lightning data and Dr. Angel Otarola in the analysis of NARR data. The authors thank Dr. David Gochis and two anonymous reviewers of the manuscript for their comments and suggestions during the revision process. The Department of Atmospheric Sciences at the University of Arizona supported this research.

REFERENCES

Adams, D. K., and A. C. Comrie, 1997: The North American monsoon. *Bull. Amer. Meteor. Soc.,* **78,** 2197–2213.

Balling, R. C., Jr., and S. W. Brazel, 1987: Diurnal variations in Arizona monsoon precipitation frequencies. *Mon. Wea. Rev.,* **115,** 342–346.

Biagi, C. J., K. L. Cummins, K. E. Kehoe, and E. P. Krider, 2007: National Lightning Detection Network (NLDN) performance in southern Arizona, Texas, and Oklahoma in 2003–2004. *J. Geophys. Res.,* **112,** D05208, doi:10.1029/2006JD007341.

Carleton, A. M., 1986: Synoptic–dynamic character of "bursts" and "breaks" in the southwest U.S. summer precipitation singularity. *J. Climatol.,* **6,** 605–623.

——, D. A. Carpenter, and P. J. Weser, 1990: Mechanisms of interannual variability of the southwest United States summer rainfall maximum. *J. Climate,* **3,** 999–1015.

Castro, C. L., T. B. McKee, and R. A. Pilke, 2001: The relationship of the North American monsoon to tropical and North Pacific surface temperatures as revealed by observational analysis. *J. Climate,* **14,** 4449–4473.

——, R. A. Pielke Sr., and J. O. Adegoke, 2007a: Investigation of the summer climate of the contiguous United States and Mexico using the Regional Atmospheric Modeling System (RAMS). Part I: Model climatology (1950–2002). *J. Climate,* **20,** 3844–3865.

——, ——, ——, S. D. Schubert, and P. J. Pegion, 2007b: Investigation of the summer climate of the contiguous United States and Mexico using the Regional Atmospheric Modeling System (RAMS). Part II: Model climate variability. *J. Climate,* **20,** 3866–3887.

Comrie, A. C., and E. C. Glenn, 1998: Principal components based regionalization of precipitation regimes across the southwest United States and northern Mexico, with an application to monsoon precipitation variability. *Climate Res.,* **10,** 201–215.

Cramer, J. A., K. L. Cummins, A. Morris, R. Smith, and T. R. Turner, 2004: Recent upgrades to the U.S. National Lightning Detection Network. *18th Int. Lightning Detection Conf.,* Helsinki, Finland, Vaisala.

Douglas, A. V., and P. J. Englehart, 2007: A climatological perspective of transient synoptic features during NAME 2004. *J. Climate,* **20,** 1947–1954.

Douglas, M. W., and J. C. Leal, 2003: Summertime surges over the Gulf of California: Aspects of their climatology, mean sounding, and evolution from radiosonde, NCEP reanalysis, and rainfall data. *Wea. Forecasting,* **18,** 55–74.

——, R. A. Maddox, K. Howard, and S. Reyes, 1993: The Mexican monsoon. *J. Climate,* **6,** 1665–1677.

Grantz, K., B. Rajagopalan, M. Clark, and E. Zagona, 2007: Seasonal shifts in the North American monsoon. *J. Climate,* **20,** 1923–1935.

Hales, J. E., 1972: Surges of maritime tropical air northward over the Gulf of California. *Mon. Wea. Rev.,* **100,** 298–306.

——, 1974: Southwestern United States summer monsoon source—Gulf of Mexico or Pacific Ocean? *J. Appl. Meteor.,* **13,** 331–342.

——, 1977: On the relationship of convective cooling to nocturnal thunderstorms at Phoenix. *Mon. Wea. Rev.,* **105,** 1609–1613.

Higgins, R. W., Y. Yao, and X. L. Wang, 1997: Influence of the North American monsoon system on the U.S. summer precipitation regime. *J. Climate,* **10,** 2600–2622.

——, W. Shi, and C. Hain, 2004: Relationships between Gulf of California moisture surges and precipitation in the southwestern United States. *J. Climate,* **17,** 2983–2997.

James, I., and B. Hoskins, 1985: Some comparisons of atmospheric internal and boundary baroclinic instability. *J. Atmos. Sci.,* **42,** 2142–2155.

Johnson, R. H., P. E. Ciesielski, B. D. McNoldy, P. J. Rogers, and R. K. Taft, 2007: Multiscale variability of the flow during the North American Monsoon Experiment. *J. Climate,* **20,** 1628–1648.

Kalnay, E., and Coauthors, 1996: The NCEP/NCAR 40-Year Reanalysis Project. *Bull. Amer. Meteor. Soc.,* **77,** 437–471.

Kelley, W. E., and D. R. Mock, 1982: A diagnostic study of upper tropospheric cold lows over the western North Pacific. *Mon. Wea. Rev.,* **110,** 471–480.

King, T. S., and R. C. Balling, 1994: Diurnal variations in Arizona monsoon lightning data. *Mon. Wea. Rev.,* **122,** 1659–1664.

Knievel, J. C., D. A. Ahijevych, and K. W. Manning, 2004: Using temporal modes of rainfall to evaluate the performance of a numerical weather prediction model. *Mon. Wea. Rev.,* **132,** 2995–3009.

Livezey, R. E., and W. Y. Chen, 1983: Statistical field significance and its determination by Monte Carlo techniques. *Mon. Wea. Rev.,* **111,** 46–59.

Maddox, R. A., D. M. McCollum, and K. W. Howard, 1995: Large-scale patterns associated with severe summertime thunderstorms over central Arizona. *Wea. Forecasting,* **10,** 763–778.

Magirl, C. S., and Coauthors, 2007: Impact of recent extreme Arizona storms. *Eos, Trans Amer. Geophys. Union,* **88,** 191–193.

Mesinger, F., and Coauthors, 2006: North American Regional Reanalysis. *Bull. Amer. Meteor. Soc.,* **87,** 343–360.

Mitchell, D. L., D. Ivanova, R. Rabin, T. J. Brown, and K. Redmond, 2002: Gulf of California sea surface temperature and the North American monsoon: Mechanistic implication from observation. *J. Climate,* **15,** 2261–2281.

Mo, K. C., M. Chelliah, M. Carrera, R. W. Higgins, and W. Ebisuzaki, 2005: Atmospheric moisture transport over the United States and Mexico as evaluated from the NCEP regional reanalysis. *J. Hydrometeor.,* **6,** 710–728.

Moore, T. J., R. L. Gall, and T. C. Adang, 1989: Disturbances along the Arizona monsoon boundary. *Mon. Wea. Rev.,* **117,** 932–941.

Murphy, M. J., and R. L. Holle, 2005: Where is the real cloud-to-ground lightning maximum in North America? *Wea. Forecasting,* **20,** 125–133.

NAME Project Science Team, cited 2004: North American Monsoon Experiment (NAME): Science and implementation plan. [Available online at http://www.cpc.ncep.noaa.gov/products/precip/monsoon/NAME.html.]

Pielke, R. A., 2002: *Mesoscale Meteorological Modeling*. Academic Press, 676 pp.

Pytlak, E., cited 2004: North American Monsoon Experiment Forecast Operations Center Plan. UCAR/JOSS. [Available online at http://www.eol.ucar.edu/projects/name/FOC_plan.html.]

——, M. Goering, and A. Bennett, 2005: Upper-tropospheric troughs and their interaction with the North American monsoon. Preprints, *19th Conf. on Hydrology,* San Diego, CA, Amer. Meteor. Soc., JP2.3.

Reyes, S., M. W. Douglas, and R. A. Maddox, 1994: El monzón del suroeste de Norteamérica (TRAVASON/SWAMP). *Atmósfera,* **7,** 117–137.

Riehl, H., 1948: On the formation of typhoons. *J. Meteor.,* **5,** 247–264.

Rogers, P. J., and R. H. Johnson, 2007: Analysis of the 13–14 July gulf surge event during the 2004 North American Monsoon Experiment. *Mon. Wea. Rev.,* **135,** 3098–3117.

Schubert, S. D., M. J. Suarez, P. J. Pegion, R. D. Koster, and J. T. Bacmeister, 2004: Causes of long term drought in the U.S. Great Plains. *J. Climate,* **17,** 485–503.

Sheppard, P. R., A. C. Comrie, G. D. Packin, K. Angersbach, and M. K. Hughes, 2002: The climate of the U.S. southwest. *Climate Res.,* **21,** 219–238.

Tapia, A., J. A. Smith, and M. Dixon, 1998: Estimation of convective rainfall from lightning observations. *J. Appl. Meteor.,* **37,** 1497–1509.

Underwood, S. J., and M. D. Schultz, 2004: Patterns of cloud-to-ground lightning and convective rainfall associated with postwildfire flash floods and debris flows in complex terrain of the western United States. *J. Hydrometeor.,* **5,** 989–1003.

Wallace, J. M., 1975: Diurnal variations in precipitation and thunderstorm frequency over the conterminous United States. *Mon. Wea. Rev.,* **103,** 406–419.

Watson, A. I., R. L. Holle, and R. E. López, 1994a: Cloud-to-ground lightning and upper-air patterns during bursts and breaks in the southwest monsoon. *Mon. Wea. Rev.,* **122,** 1726–1739.

——, ——, and ——, 1994b: Diurnal cloud-to-ground lightning patterns in Arizona during the southwest monsoon. *Mon. Wea. Rev.,* **122,** 1716–1725.

Watts, C. J., R. L. Scott, J. Garatuza-Payan, J. C. Rodriguez, J. H. Prueger, W. P. Kustas, and M. Douglas, 2007: Changes in vegetation condition and surface fluxes during NAME 2004. *J. Climate,* **20,** 1810–1820.

Whitfield, M. B., and S. W. Lyons, 1992: An upper-tropospheric low over Texas during summer. *Wea. Forecasting,* **7,** 89–106.

Zajac, B. A., and S. A. Rutledge, 2001: Cloud-to-ground lightning activity in the contiguous United States from 1995 to 1999. *Mon. Wea. Rev.,* **129,** 999–1019.

Zehnder, J. A., 1993: The influence of large-scale topography on barotropic vortex motion. *J. Atmos. Sci.,* **50,** 2519–2532.